ChemistrySelect
Chemistry Europe
European Chemical Societies Publishing

RESEARCH ARTICLE

# Biogenic-Assisted Synthesis of Cu–Zn–Co Ternary Oxides Nanocomposite: Investigation on Their Bioactivity and Electrochemical Behavior

Sheikdawood Parveen[1] | Baskar Anbumani[2] | Manickam Karthigai Priya[3] | Punniyakotti Parthipan[4] | Gnanasekaran Lalitha[5] | Ayyar Manikandan[2,6] | Arumugam Kosiha[7] | Giriraj Kalaiarasi[2,6]

[1]Bio-Inspired Material Research Laboratory, Dr. Mahalingam College of Engineering and Technology, Coimbatore, Tamil Nadu, India | [2]Department of Chemistry, Karpagam Academy of Higher Education (Deemed to Be University), Coimbatore, Tamil Nadu, India | [3]Department of Science and Humanities, Rathinam Technical Campus, Coimbatore, Tamil Nadu, India | [4]Department of Biotechnology, Faculty of Science and Humanities, SRM Institute of Science and Technology, Kattankulathur, Chengalpattu, Tamil Nadu, India | [5]Instituto de Alta Investigación, Universidad de Tarapacá, Arica, Chile | [6]Centre For Material Chemistry, Karpagam Academy of Higher Education (Deemed to Be University), Coimbatore, Tamil Nadu, India | [7]Department of Chemistry, VELS Institute of Science, Technology & Advanced Studies (Deemed to Be University), Chennai, Tamil Nadu, India

**Correspondence:** Arumugam Kosiha (kosiha.sbs@velsuniv.ac.in) | Giriraj Kalaiarasi (kalaiarasi.giriraj@kahedu.edu.in)

**Received:** 17 September 2025 | **Revised:** 26 January 2026 | **Accepted:** 29 January 2026

**Keywords:** Antioxidant activity | copper zinc cobalt oxides | Electrochemical performance | Facile synthesis | *Myristica fragrans* (nutmeg) mace extract | Nanocomposite (NAC)

## ABSTRACT

Nanoparticles are the materials of the future after their well garnished development, especially, in the field of biomedical and energy sectors because of its qualitative priority of people. By spotting these aspects, we determine to synthesize a mixed metal oxide appended nanocomposite (NAC) from Cu, Zn and Co. We eradicate the utilization of chemicals by plant-assisted synthetic approach. In this method we employs the aqueous extract from *Myristica fragrans* (nutmeg) mace as a reducing, capping and stabilizing agent to synthesize the mixed metal oxide-based nanocomposite composed of Cu, Zn, and Co. FT-IR, UV–Visible, PXRD, scanning electron microscopy (SEM), EDS, and transmission electron microscopy (TEM) techniques supports the formation of desired NAC in both morphologically and chemically. The antioxidant activity of the NAC was assessed against the $DPPH^{\bullet}$, $ABTS^{\bullet+}$, $NO^{\bullet}$, ferric reducing antioxidant power (FRAP), and $O^{2-}$ free radicals. Further, the electrochemical properties of CV, GCD and EIS are measured in 6 M NaOH. At a 1 $Ag^{-1}$ current density, the composite exhibit greater capacitance (402.04 C $g^{-1}$), after 2000 cycles the NAC electrode shows excellent 95% of capacity retention.

## 1 | Introduction

Nanoparticles possess excellent physical, chemical and biological properties than their bulk counter parts due to their high surface area to volume ratio, surface energy and quantum effects. Due to this difference in their properties, they have vast and efficient applications in energy, biomedical, and other fields too [1–3]. Nanometal oxides were the class of nanomaterials having the bond between or among metal ion and oxygen atom. Ternary metal oxides were the class of nanomaterials which were always superior than the bi or mono metal oxides because they have enhanced redox and surface activity.

The mixed metal oxide-based nanoparticles were very useful in designing the energy storage related applications. They show diversified oxidation states; this enables the faradic reactions

that promotes pseudo capacitance [1]. Greenly synthesized metal oxides exhibit superior catalytic activity because of tailored morphology and active sites [4]. The improved synergistic properties of mixed metal oxides enhance their biological properties like anticancer, antioxidant, antifungal, and antibacterial. Ternary metal oxides have high surface area, porosity, biocompatibility and low toxicity [5–7]. Nanoscale size and porous structure has greater active surface sites for antioxidant reactions [4].

Utilization of the antioxidant potential of the nanoparticles were useful in many aspects like combatting the oxidative which is major impactor to neural disorders, cancer, cardio diseases and aging in humans. How the NP's especially metal oxides comprise of zinc, cerium, and gold useful was, they can mimic the natural antioxidant enzymes like superoxide dismutase (SOD) and catalase, neutralizing the harmful reactive oxygen species (ROS) effectively [8]. The redox reactive surfaces of metal oxides enable them to scavenge the free radicals and making them as the promising agents for therapeutic applications which revolves around the oxidative stress related applications [9]. As a comparison, traditional antioxidant continuously suffer from bioavailability, instability to cross the barriers in human body (blood–brain barrier), studies proven that nano oxidants can cross the blood–brain barrier and prevents neuron from oxidative stress. Nano oxidants deliver merits like targeted drug delivery, sustained release and enhanced cellular uptake making them efficient at therapeutics [10–13].

Copper metal has a privilege to switch between the oxidation states ($Cu^{+}$ and $Cu^{2+}$) enabling enhanced electron donation. This electron donation will neutralize the free radicals. Cu-based mixed metal oxide nanocomposites (NACs) have superior radical scavenging activity at DPPH and ABTS assays. Zinc contributes to the stability and biocompatibility whereas copper contributes to the redox cycling and radical scavenging [5, 14]. Cobalt also exists in $Co^{2+}$ and $Co^{3+}$ oxidation states, which allows it to take part in the redox cycling and exhibits excellent scavenging activity by donating and accepting electrons [15]. Cobalt was combined with other metals shows enhanced electron transfer, surface area and catalytic activity, as a collective result improves the radical scavenging efficiency and stability [16]. Cobalt-based metal oxides maintain structural nature under the physiological conditions, which makes them best suitable for antioxidant applications [15, 16].

Till today many metal oxides and mixed metal oxides-based NACs were undergone many antioxidant and other biological applications [17–24]. Bavaji et al. synthesized the NAC of $ZrO_2$/NiO/RGO for antioxidant applications as part of study [17]. El-Shafai et al. reported the NAC GO@$TiO_2$.ZnO and studied their antioxidant applications [18]. Jahanzeb Khan et al. presented the ternary metal oxide NAC (CuO/NiO/ZnO) for the antioxidant and antimicrobial applications [19]. Athithyan et al. synthesized the mixed metal oxide of CoO/NiO from green synthesis for trifunctional applications includes antioxidant applications [20]. Ruthiran Papitha et al. synthesized two nanocomposites by using the bark extract of *Parkia timorina*. They synthesized CuO/$TiO_2$ and ZnO/$TiO_2$ and comparatively studied their antioxidant potential [23].

Plant extracts play a vital role in preparing a metal oxide and mixed metal oxides nanoparticles. The authors synthesized CuO/ZnO/CoO NACs using nutmeg mace extracts. The extract of nutmeg (*Myristica fragrans*) mace (outer layered flower of nutmeg) was used as precursor to synthesis composite. Biogenic precursors in the extract's functional groups such as flavonoids, terpenoids improves the dispersion, stability, and surface reactivity of composites [25, 26]. Further, we can rule out the use of chemicals used for the synthesis which were harmful for environment, this reduces environmental pollution, energy consumption and hazardous by products [27, 28]. The Phytochemicals in the plant extract plays the role of reducing agent which reduces the metal ions to their corresponding metal or metal oxide NP's and as well as role of stabilizers and capping agents by binding to the nanoparticle surface, preventing agglomeration and controlling particle size and shape. This enhances colloidal stability and biocompatibility [29, 30]. Even though biological capping agents were not that much good as chemical capping agents but in the case of chemical capping agents change in the small ratio results in large variation in morphology of nanostructures. Biogenic (plant-based) capping agents are cost-effective because they use readily available, inexpensive natural materials and simple processing, making them a more economical alternative to conventional chemical capping agents. Plant extracts are rich in phytochemicals. Plant extracts act as capping agents by providing bioactive molecules that bind to newly formed nanoparticles, preventing them from clumping through steric hindrance and electrostatic repulsion, while simultaneously reducing metal ions to form the nanoparticles, creating a stable, eco-friendly synthesis method and their rate of synthesis was also faster. The nanoparticles synthesized by plant extract have better biological properties [31, 32].

This plant-assisted synthesis route is much cheaper compared to conventional chemical routes. The main cost advantages come from the fact that inexpensive, locally sourced plant material acts both as a reducing agent and a stabilizing agent, and there is no need for toxic reagents, elaborate purification, and waste management. Energy input is also reduced due to milder synthesis conditions. Literature and process analyses estimate total expensive for plant-mediated mixed metal oxide nanoparticle synthesis to be 30%–70% lower per gram compared to chemical synthesis, with additional environmental and safety benefits [33, 34].

In this research work we synthesized the mixed metal oxides of Cu, Zn, and Co (NAC) using the nutmeg mace extract. We studied the antioxidant potential of the mixed metal oxide NAC in the free radicals of $DPPH^{\bullet}$, $ABTS^{\bullet+}$, $NO^{-}$, ferric reducing antioxidant power (FRAP), and $O^{2-}$ free radicals. Being the environmentally friendly and owning the potential antioxidant activity this Cu—Zn—Co metal oxides can be considered as a potent candidate for antioxidant application. Further, electrochemical properties of the NAC were also investigated.

## 2 | Experimental Section

### 2.1 | Plant Identification and Its Phytochemical Constituents

Initially the tree of the nutmeg and mace was identified and it was belongs to the family of *Myristicaceae*. It was tropical tree

with soft wooded aromatic characteristics. Also, used in Indian cooking as the spice. It can grow up to height of about 10–20 m tall with straight trunk and canopy (dense). Leaves were alternatively arranged, simple and oblong-lanceolate shaped. It was a dioecious tree. *M. fragrans arils* (mace) holds distinct variety of phytochemicals in nature. Seed (nutmeg) contains majorly myristicin and safrole. Arils (mace) comprises of many phytochemical constituents and essential oils which includes flavonoids like quercetin, quercetin-3-*o*-glucoside, rhamnetin, rutin, lutein, and procyanidin B2; phenolic acids like ferulic acid and vanillic acid; terpenoids like myristicin, elemicin, and safrole and other lignans and tannins [35, 36].

Many reviews and experimental research works in nanoparticle syntheses suggests us that plant extracts were like bio factories; they reduce the metal precursors and also acts as a capping agent. On the other hand, plant extracts help eliminate the use of toxic chemical reagents in the synthesis of nanoparticles. Mace is enriched in phenylpropanoids like myristicin, flavonoids and tannins. They donate electrons to reduce the metal ions from their higher oxidation states and gives the caps them and controls the agglomeration of NACs. Compared to other spices arils contains higher small-molecule antioxidant density and lower polysaccharide burden which favors the thinner and uniform organic shells on nanoparticles and improves dispersion. Reduction of metal precursors was taken care by polyphenols and phenylpropenes in mace they donate electron to metal ions and reduces and initiates the nucleation process. Phenolic -OH groups and aromatic rings adsorb at nascent particles surface and limits the coalescence and impacts the morphology [37, 38].

The phenolics reduce metal ions during nucleation and immediate adsorption caps nuclei and limits the uncontrolled growth. Acidic and phenolic groups give negative charge and increases the zeta potential and colloidal stability was maintained via electrostatic repulsion. Bulky phytochemicals like tannins creates a barrier around nanoparticles. The steric hindrance reduces the van der waals force of attraction and flocculation and caps the nanoparticles [36, 39, 40].

## 2.2 | Preparation of Plant Extract

Ripened fruits of Nutmeg were collected from Pollachi region, Tamil Nadu, India. From the sourced nutmeg fruit, hand removing of the crimson mace (nutmeg mace) was carried out carefully and dried in sunlight for about 12 days to get a yellowish orange color mace. Dried nutmeg mace was stored in an airtight container for future use. The 10 g dried and crushed nutmeg mace was added into a conical flask of 250 and 100 mL of deionized water was added into the crushed mace nutmeg. It was placed in a water bath for 3–4 h at 85°C. Then the contents in the flask was filtered through Whatman No.1 filter paper. Then the extract was cooled at 25 ± 1° C for 180 min and used as such.

## 2.3 | Preparation of Cu—Zn—Co Metal Oxide (NAC)

Each one molar (1 M) solutions of copper nitrate $Cu(NO_3)_2.3H_2O$, zinc nitrate $Zn(NO_3)_2.6H_2O$, and cobalt nitrate $Co(NO_3)_2.6H_2O$ was prepared by using 50 mL of nutmeg mace extract. For synthesis of NAC, all three metal nitrate solutions were taking them in equimolar ratio as 1:1:1. Then, metal salt solutions were thoroughly mixed well and kept for stirring, to this few drops of 0.2 M NaOH was added and continued stirring for about 10 h at an ambient temperature. The resultant precipitate was filtered through a Whatman no. 1 filter paper. The dried material was calcinated in a muffle furnace at 600°C for 4 h. After the calcination the NAC was obtained and utilized for further analysis.

## 2.4 | Characterization of NAC (Cu—Zn—Co Oxide NAC)

The structural properties of NAC were assessed through various instrumental techniques. Detailed instrumentation was mentioned in Supporting Information.

## 2.5 | Antioxidant Assays

Antioxidant activity of the NAC was tested according to the reported literature methods [41–50]. Antioxidant activity of the composite was assessed using various well-known assays which includes DPPH• (2,2-diphenyl-1-picrylhydrazyl) assay is to compare the antioxidant strength in natural products, pharmaceuticals and nanomaterials, ABTS•+ (2,2'-azino-bis(3-ethylbenzothiazoline-6-sulfonic acid) assay was used to assess the total antioxidant capacity of the nanomaterial it was very versatile and works in both lipids and aqueous systems, NO• (nitric oxide) radical scavenging assay is kept in place to check whether our NAC reduce inflammation signaling because NO• is significant cause for inflammation, neurodegeneration and cancer progression and $O^{2-}$ (Super Oxide anion) assay was used to assess the mitochondrial protection and antiaging affects and it was a key parameter to oxidative stress and mitochondrial dysfunction and acts as a marker to cell protective activity, FRAP used to measure the antioxidant capacity of a sample by its ability to reduce ferric ($Fe^{3+}$) ions to ferrous ($Fe^{2+}$) ions and it offers a simple and efficient analytical method for assessing age, disease, diet, or other physiological changes to antioxidant status. The free radicals used in the testing of antioxidants activity of NAC were DPPH•, ABTS•+, NO•, $O^{2-}$, FRAP at varying concentrations and detailed experimental procedure was provided at Supporting Information. Assuring consistency, all experimental measurements were carried out in triplicate ($n$ = 3). Three independent replicates are used to calculate the mean ± standard deviation (SD), which is how quantitative data are reported.

## 2.6 | Electrochemical Performance

Electrochemical behavior of NAC was systematically estimated using cyclic voltammetry (CV) and galvanostatic charge/discharge (GCD) and electrical impedance spectroscopy (EIS). In CV the difference between capacitance and diffusion-controlled contributions were measured. GCD is used to calculate the specific capacitance and evaluate the rate capability and cyclic stability. EIS provides mechanistic data values

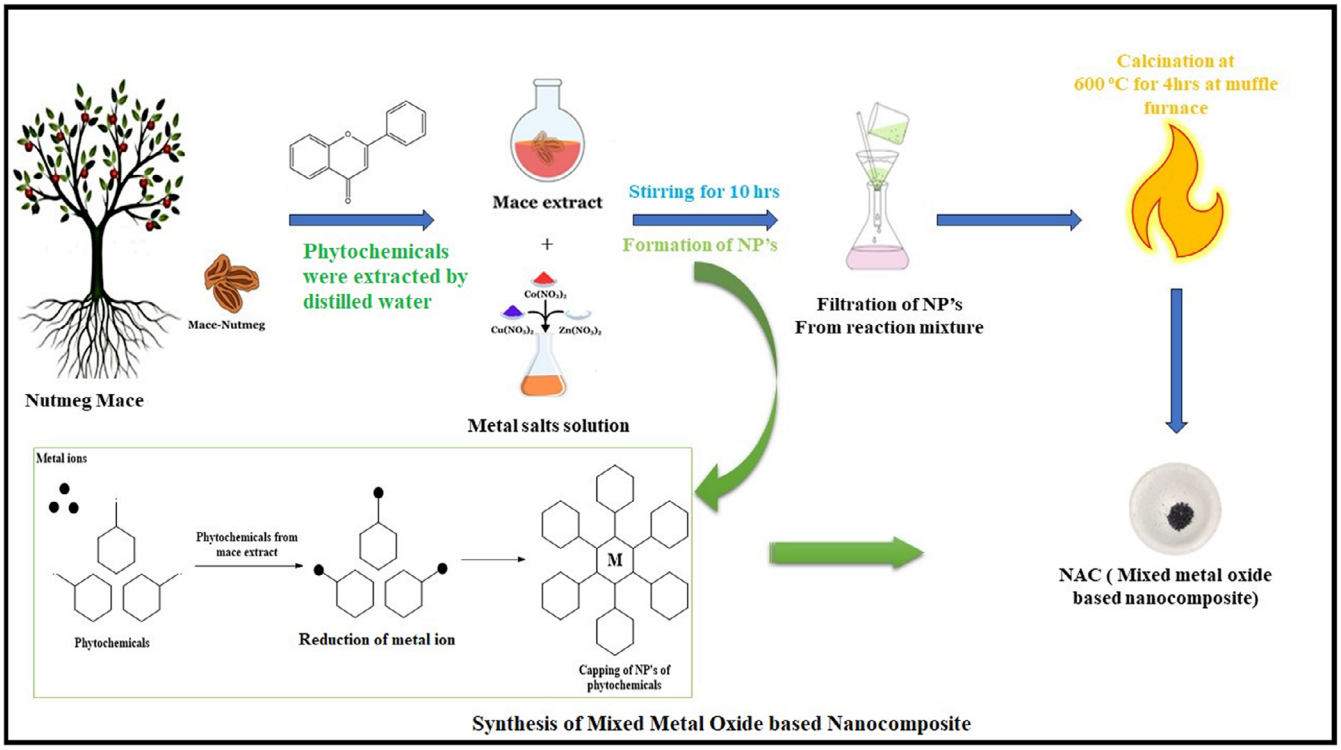


**SCHEME 1** | Preparative route of the NAC.

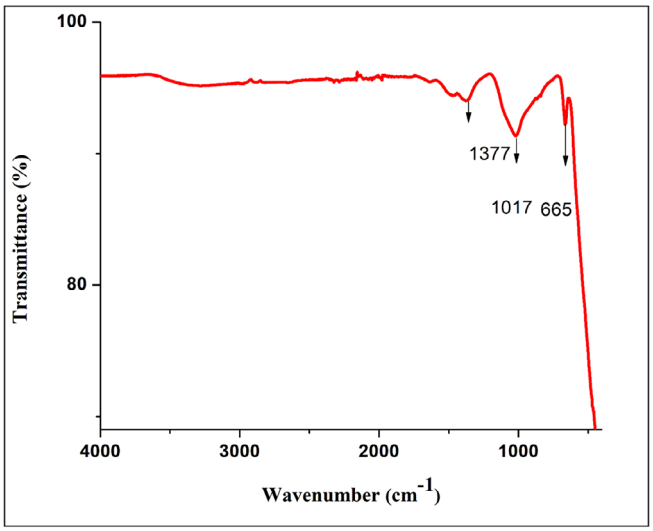


**FIGURE 1** | FT-IR spectrum of NAC composite.

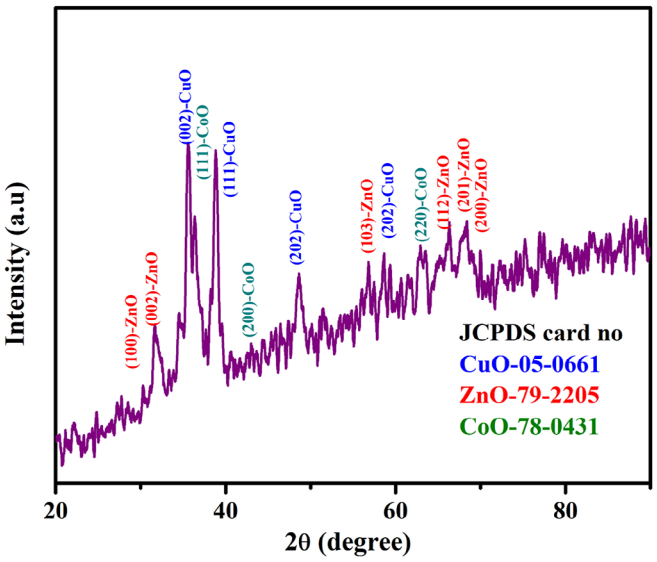


**FIGURE 2** | PXRD pattern of the NAC.

into charge transfer resistance and ion diffusion pathways [51–53]. The measurements were carried out at the CH1608 electrochemical work station by using the 6 M KOH electrolyte in three electrode configuration model. 50 milliliters of *N*-methyl-2-pyrrolidone (NMP) solvent were added to the mixture of active material (75%), carbon black (15%), and polyvinylidene difluoride (PVDF) (PVDF was used as nothing but a binder). The graphite sheet with a dimension of 1 × 1 $cm^2$ was used as the current collector and covered with the 1 mg of electrode material (NAC), then it was dried for 8 h at 80°C in this work the standard electrode was Ag/AgCl and the counter electrode was Pt wire.

The GCD profile was used to calculate the specific capacitance (Sc) by Equation (1):

$$C = \frac{I \times \Delta t}{m \times V} \quad (1)$$

where, $I$ is current, $\Delta t$ is discharge current, $V$ = voltage, and $m$ = mass of material.

## 3 | Results and Discussion

The synthesis of metal oxides by using the plant's found its own space in the nanomaterial field due its ease in synthesis and effectiveness in research. The NAC was synthesized by using the nutmeg mace extract and nitrate salts of copper, zinc and cobalt. The resultant mixture (dried NAC) was calcinated at 600°C to remove the organic and inorganic contaminants from the NAC (Scheme 1). The nutmeg mace extract was used as capping, stabilizing and chelating agent helps in the effective formation of NAC [25]. Reported research works reveals that presence of adequate amounts of phytochemicals (myristicin, eugenol, elemicin, safrole, lignans, flavonoids, phenolic acids, terpenoids, tannins, and alkaloids) in the extract of *M. fragrans* [39, 54, 55]. The various roles of these phytochemicals in synthesis of NAC were Lignans in stabilization, Flavonoids as reducing and capping agent, Phenolic acids as surface passivator, aggregation preventer and dispersion improvisor, Terpenoids will be shape control and surface stabilization, Tannins as chelation and capping agent, Alkaloids used in surface modification and stabilization [56–59]. The mechanism for the formation of NAC was elucidated by using the previous literature methods and its graphical representation was presented in the Scheme 1 [60, 61].

### 3.1 | Spectral Characterization of NAC

#### 3.1.1 | FT-IR Analysis for NAC nanocomposite

To explore the formation of NAC, the FT-IR spectra of *M. fragrans* and NAC was compared. *M. fragrans* shows the bands in the wavenumbers of 3434, 2810, 1642, 1387, 1345, and 673 $cm^{-1}$ was due to the presence O—H stretching hydrogen, C—H stretching, HC═C alkene peak, C—H stretching and C—F stretching, respectively [62]. Plant-assisted synthesis of NAC showed bands in the regions of 1376 $cm^{-1}$ was due to the presence of bending vibration of surface hydroxyl group and the peaks observed at 1017 and 665 $cm^{-1}$ were due to the metal–oxygen/metal–metal vibrations, respectively [62, 63]. The IR bands in the NAC contain few bands when compared to IR bands *M. fragrans* this was the evidence for the formation of NAC. This shows the complete removal of both the organic and inorganic contaminants (Figure 1).

#### 3.1.2 | UV–Visible Spectroscopy

The reduction of the metal ions to the metal oxide state was identified using the UV–Visible spectroscopy. The UV–vis spectrum of NAC and band gap energy ($E_g$) was presented in Figure S1. The NAC shows peak in the wavelength of 369 nm which is due to the metal–oxygen transition, which evidenced the reduction of metal ions to form the NAC [64]. The $E_g$ of the spectrum was found to be 3.43 eV [65].

#### 3.1.3 | Powder X-Ray Diffraction Analysis (PXRD)

The PXRD characterization technique was employed to know the phase purity of the samples applied for the analysis under the testing environment. Figure 2 contains the powder XRD pattern of the NAC. The characteristic peaks at $2\theta = 31.7$, 34.6, 35.5, 36.3, 38.9, 43, 48.6, 56.7, 58.4, 62.5, 63.4, 66.2, and 68.2, which were corresponded to CuO, ZnO, and CoO nanoparticles. The CuO has the peaks and assignments as 35.5 (002), 48.6 (202) and 58.4 (202) this was in line with the JCPDS card. no. 05-0661. For ZnO 31.7 (100), 34.6 (002), 36.3 (101), 56.7 (103), 63.4 (112), 66.2 (201), and 68.2 (200), whereas CoO have $2\theta$ value and assignments as 38.9 (111), 43.0 (200), and 62.2 (220). The crystallite size of NAC was found to 17.75 nm by using the Debye–Scherrer's formula. The PXRD data for the synthesized NAC was presented in Tables 1 and 2.

**TABLE 1** | PXRD data for the NAC.

| Metal oxide | Peaks | Assignments | JCPDS card no. |
|---|---|---|---|
| CuO | 35.5 | 002 | 05-0661 |
| | 48.6 | 202 | |
| | 58.4 | 202 | |
| ZnO | 31.7 | 100 | 79-2205 |
| | 34.6 | 002 | |
| | 36.3 | 101 | |
| | 56.7 | 103 | |
| | 63.4 | 112 | |
| | 66.2 | 201 | |
| | 68.2 | 200 | |
| CoO | 38.9 | 111 | 78-0431 |
| | 43.0 | 200 | |
| | 62.2 | 220 | |

Average crystallite size of the particles calculated from the Debye–Scherrer's equation (Equation 2) [66, 67].

$$D = \frac{K\lambda}{\beta \cos\theta} \tag{2}$$

where, $D$ is the average crystallite size in nanometers, $K$ is the shape factor (0.9), $\lambda$ is the wavelength of the x-rays, $\beta$ is the peak broadening in radians at half of the maximum intensity (FWHM) $\theta$ is the Bragg angle in radians. The average crystallite of NAC was found to 17.03 nm (Table 2). Dislocation density ($\delta$) is the number of dislocations per unit volume and can be estimated from the crystallite size [68] (Equation 3).

$$\delta = \frac{1}{D^2} \tag{3}$$

Where, $D$ is the average crystallite size in nanometers. The dislocation density is $8.09\times10^{-3}$ $nm^{-2}$. This microstrain rises from the large fraction of exterior atoms and unsaturated affecting bonds, which may be responsible for really a lot of unique chemical and physical properties of the nanoparticles. Microstrain (ε)

**TABLE 2** | Crystallite size, dislocation density, and microstrain for the NAC.

| Peak position $2\theta$ (°) | FWHM $\beta$ (°) | Crystallite size | Dislocation density | Microstrain |
|---|---|---|---|---|
| 27.46258 | 0.2 | 38.5711639 | 0.672162859 | 3.57133691 |
| 35.89205 | 1.1 | 6.86803061 | 21.19998508 | 14.8193077 |
| 38.82095 | 0.2 | 37.4491636 | 0.713043055 | 2.47662023 |
| 48.63925 | 0.95 | 7.61738045 | 17.23410387 | 9.17212728 |
| 62.70243 | 0.56 | 12.1102389 | 6.818590073 | 4.01070674 |
| 62.70243 | 0.52 | 13.0417957 | 5.879294502 | 3.72422769 |
| 66.46453 | 0.65 | 10.2191675 | 9.575665387 | 4.32878455 |
| 67.73196 | 0.45 | 14.6531514 | 4.657339791 | 2.92574049 |
| 58.59263 | 0.54 | 12.825041 | 6.079704607 | 4.19932202 |
| Average | | 17.0394592 | 8.092209915 | 5.46979707 |

calculated from the following relation [69] (Equation 4):

$$\varepsilon = \frac{\beta}{4\tan\theta} \tag{4}$$

The material's micro strain value was found to be about $5.46\times 10^{-3}$.

### 3.1.4 | Scanning Electron Microscopy (SEM)

Scanning Electron Microscopy is the analysis use to know the surface morphology of the nanomaterials at various magnifications which was presented below as Figure 3. at the magnifications of 500 nm and 1 μm. The in consistent spherical shape and some layer shape of NAC were identified in the SEM scans. This shows that the clusters resemble amorphous aggregates these were the agglomerated particles of NAC. The reason for the agglomeration was may be due to the magnetic interactions or may be due to the phytochemicals which works as a reducing agent in the plant extract or nucleation effect [64, 70, 71].

### 3.1.5 | Energy Dispersive Spectral Analysis

Energy dispersive spectroscopy (EDS) is the characterization technique use to confirm the elemental composition of the material. EDS spectrum was shown in the Figure 4. Ranges from 0 to 20 KeV, the spectral peaks in the EDS spectrum shows that mixed metal oxide (NAC) comprises of Cu, Zn, Co, and oxygen atoms. Atomic metal composition in the NAC was given in Table 3 indicated that Co (12.79), Zn (22.29), and Cu (42.45) with oxygen (22.48) percentage, respectively. Nanoparticle compositional of NAC was indicated by EDS spectra, were matching with the theoretical values.

### 3.1.6 | Transmission Electron Microscopy (TEM)

TEM images of NAC were presented below as Figure 5. TEM images of NAC show that most of the particles are transparent, which is the proof for the formation of metal–oxygen bond. Even though, many thickened particles were identified this was may be due to the agglomeration of the particles. The selected area electron diffraction (SAED) shows significant ring like characteristics. This further enhances their polycrystalline nature. The TEM micrograph presented in Figure 6 clearly reveals that the nanostructured morphology of the synthesized particles, which appear predominantly spherical in shape. The particle sizes range from 10 to 25 nm. As indicated by the particle size distribution in Figure 7, the majority of particles fall within the 10–12 nm range. The distribution curve fits well with a log-normal function, which is typical for nanoparticle systems. The weighted average particle size obtained from the distribution is approximately 12.04 nm.

### 3.1.7 | Biological Applications: Antioxidant Studies

One of the most important investigations of nanomaterials in biomedical application system is the evaluation of their antioxidant activity [72]. Every biosystem's performance is significantly impacted by antioxidants [73]. Because of the interaction between the system's biomolecules and molecular oxygen, free radicals are frequently produced in biological systems [74]. Before being applied in real time to any living system, the antioxidant activity of synthetic nanomaterials has been assessed. In the antioxidant assays, $IC_{50}$ is the antioxidant concentration required to obtain 50% radical inhibition. In vitro antioxidant assays such $DPPH^{\bullet}$, $ABTS^{\bullet+}$, $NO^{\bullet}$, $O^{2-}$, and FRAP was performed and the results were discussed herein detail (Figure 8).

Experiments that employ DPPH radicals to evaluate the antioxidant qualities of recently created materials frequently employ the DPPH scavenging assay. Additionally, it is frequently used to assess the overall antioxidant capacity and the ability to scavenge free radicals by donating hydrogen atom. Antioxidants' ability to scavenge free radicals has long been tested using the uncharged DPPH free radical, which may be changed into a non-radical form by absorbing an electron or a hydrogen atom in the presence of a composite nanomaterial [75, 76]. In this current study, the antioxidant activity of NAC at different concentrations (20 to 100 $\mu g\ mL^{-1}$) was determined by DPPH radical scavenging assay, and

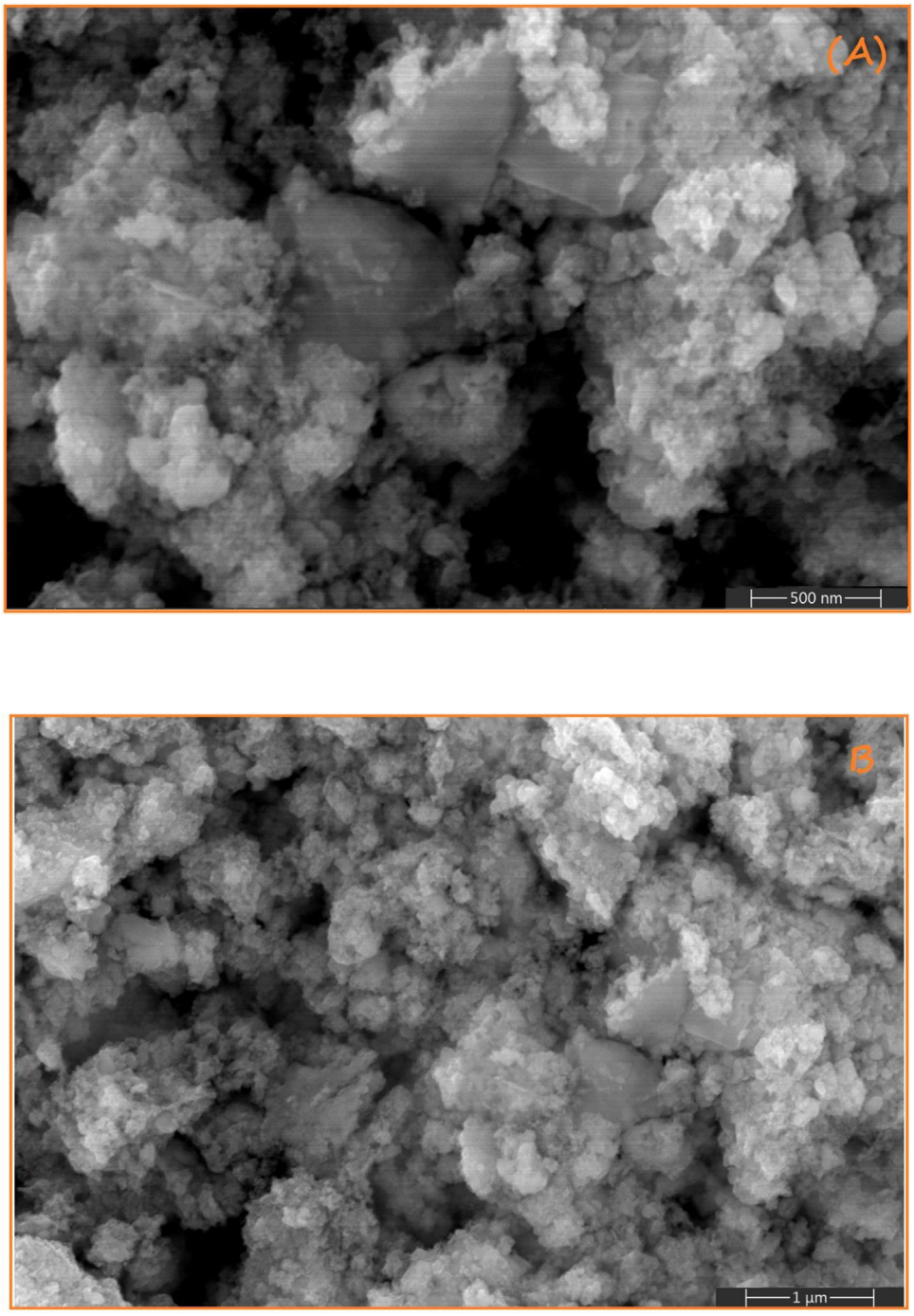


**FIGURE 3** | SEM images of NAC.

**TABLE 3** | The elemental composition of the NAC.

| Elements | Line type | *k* Factor | Absorption correction | Wt% | Wt% sigma | Atomic % |
|---|---|---|---|---|---|---|
| **O** | K series | 2.020 | 1.00 | 22.48 | 0.28 | 53.40 |
| **Co** | K series | 1.185 | 1.00 | 12.79 | 0.19 | 8.25 |
| **Cu** | K series | 1.247 | 1.00 | 42.45 | 0.29 | 25.39 |
| **Zn** | K series | 1.277 | 1.00 | 22.29 | 0.25 | 12.96 |
| Total | | | | 100.00 | | 100.00 |

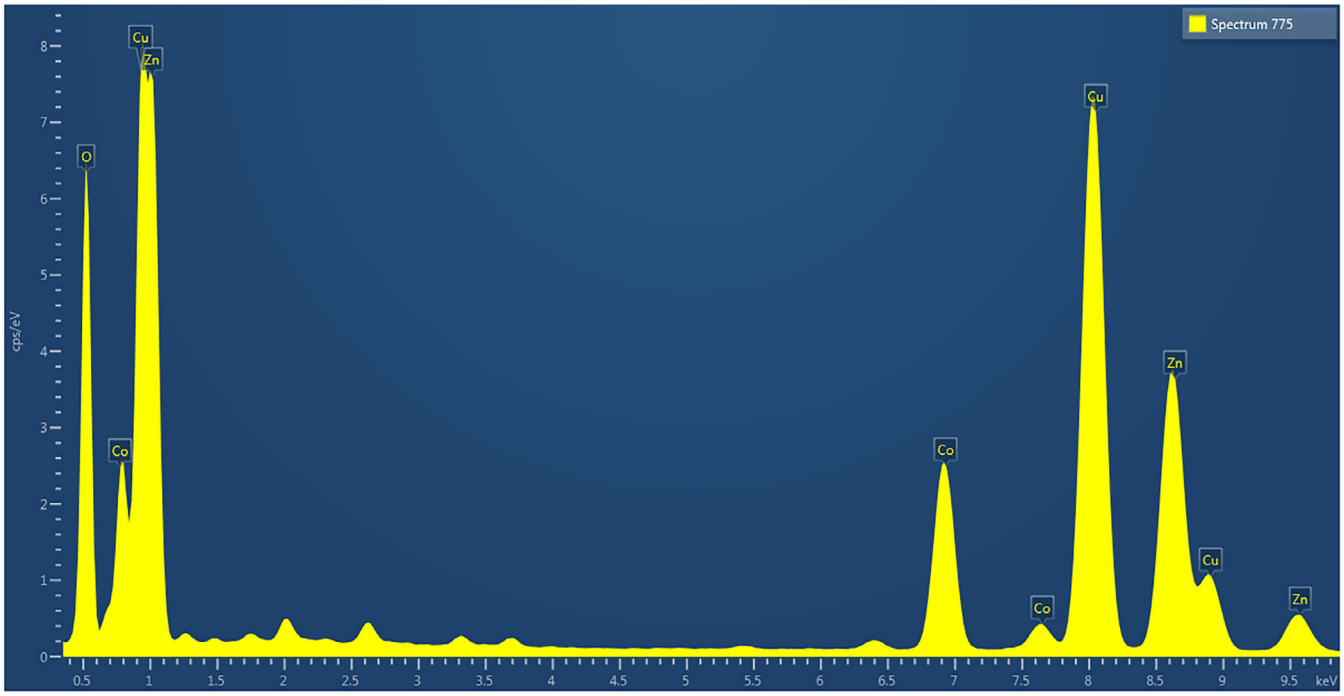


**FIGURE 4** | EDS spectrum of NAC.

the obtained result is illustrated in Figure S2. It was observed that composite (NAC) exhibited better ability to scavenge DPPH radicals, with the $IC_{50}$ value of 62.11 ± 0.15 μg $mL^{-1}$ comparable to that of AA (7.98 ± 0.98 μg $mL^{-1}$) and BHA (8.11 ± 1.12 μg $mL^{-1}$).

By testing against the $ABTS^{\cdot+}$ solution, with the increase in concentration, the percentage radical scavenging activity increased. NAC displayed scavenging activity spanning from 22.75% to 72.42% at different concentrations (Figure S3). The antioxidant capacity may be explained by the negatively charged electron-donating surface, which may be in charge of containing the ABTS free radical species [77]. As it was able to combine more ROS, the antioxidant activity was stronger [78]. The $IC_{50}$ value was calculated to be 53.5 ± 0.89 μg $mL^{-1}$ and 47.6 ± 0.11 μg $mL^{-1}$ for the controls AA and BHA, respectively, for the composite nanomaterial (NAC) it was resulted as 65.53 ± 0.49 μg $mL^{-1}$.

Scavenging Nitric Oxide (NO) refers to the process where a substance, like a composite oxide, interacts with nitric oxide and prevents it from causing damage or from being converted into more harmful reactive species. Present study shows the composite nanoparticles had nitric oxide scavenging activity. The scavenging activity of the nanoparticles was lesser as compared to standard ascorbic acid (Figure S4). The $IC_{50}$ values of controls AA and BHA additionally, NAC was estimated as 51.9 ± 0.56 μg $mL^{-1}$, 50.2 ± 0.45 μg $mL^{-1}$, and 52.12 ± 0.65 μg $mL^{-1}$ which nears the scavenging activity of the controls.

Super oxide is biologically important as it can form singlet oxygen and hydroxyl radical. Overproduction of super oxide anion radical contributes to redox imbalance and associated with harmful physiological consequences. The $IC_{50}$ of compound was 52.51 ± 0.95 μg $mL^{-1}$, indicating the better scavenging ability of the composite. Whereas, the controls showcased the free radical scavenging activity as 35.40 ± 0.56 μg $mL^{-1}$ and 42.6 ± 0.23 μg $mL^{-1}$ for AA and BHA, respectively (Figure S5).

Subsequently, FRAP of NAC was measured by the colorimetric detection to directly measure the reducing power of the compound which mirrors their power neutralize the oxidative stress. Figure S6 shows the FRAP results of the prepared composite NPs by reducing $Fe^{3+}$ ions to $Fe^{2+}$ ions. Blue color develops after the reduction of the ferric iron and it can be monitored colorimetrically at 594 nm. It was found that the maximum antioxidant activity value of 63% was observed for NAC while 91% and 81% activity was observed for AA and BHA, respectively at same concentration. This method is based on the reduction of $Fe^{3+}$ ions into $Fe^{2+}$ ions through the antioxidant (CuO, ZnO, and $Co_3O_4$ NPs) the reaction is detected by the transfer from the yellow color of $Fe^{3+}$ ions to the blue $Fe^{2+}$ ions. The increase in absorbance with concentration indicates the elevation of the reducing power of the tested samples [79, 80]. The antioxidant activity of the other reported metal oxide-based NACs which were synthesized by using plant extract was compared with NAC and the obtained results revealed that NAC possessed significant activity [79–85].

### 3.1.8 | Electrochemical Performance of NAC

The synergistic effect of CuO, CoO and ZnO, often in the form of heterostructures or composites, improves parameters like specific capacitance, energy density, power density, and cycling stability. The electrochemical performance of composite was investigated using a three-electrode configuration with a 6 M NaOH electrolyte solution as the electrolyte, Ag/AgCl serving as the reference electrode and Pt serving as the counter electrode. The CV curves of the composite electrode recorded at a scan

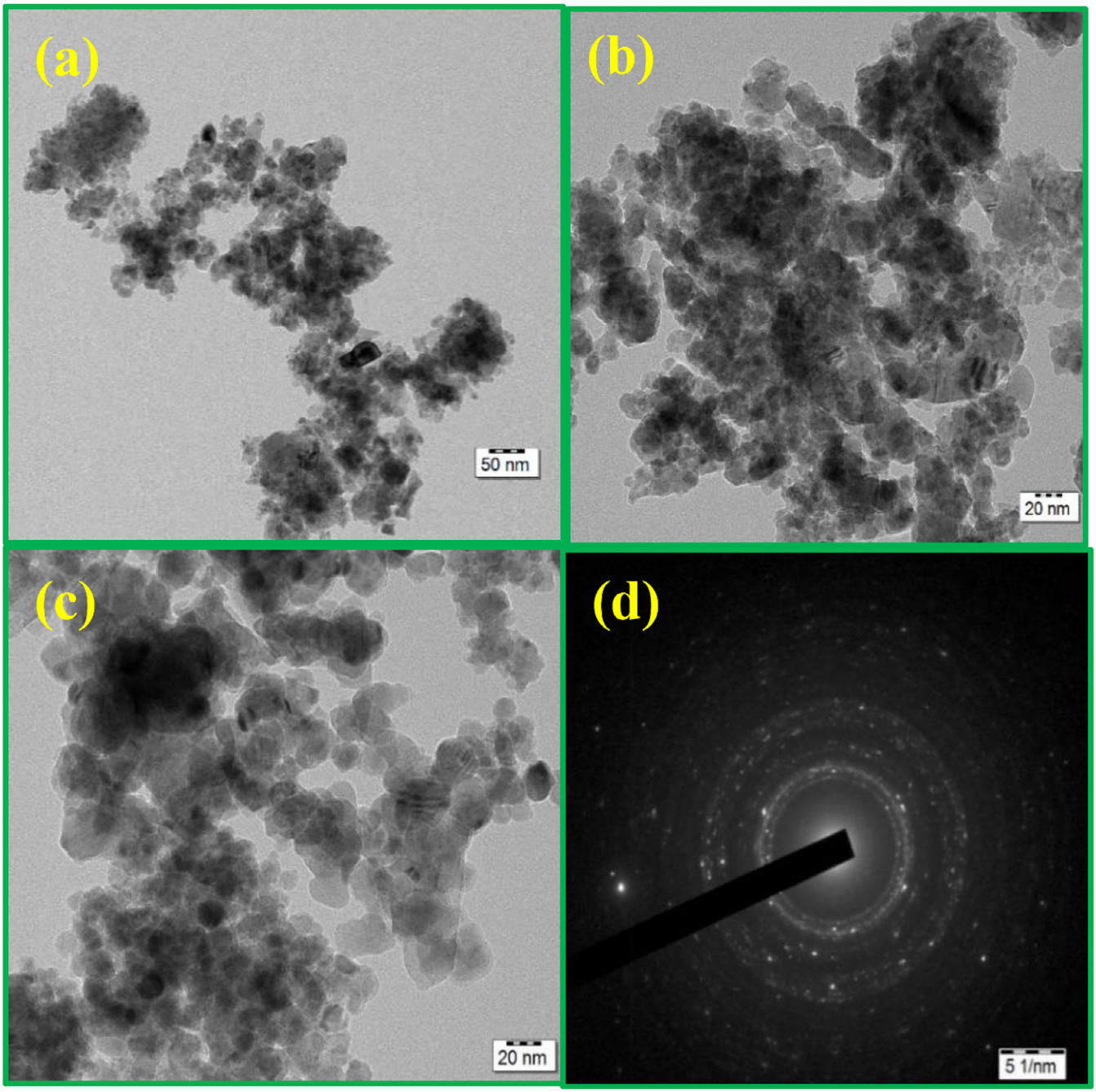


**FIGURE 5** | (a–c) TEM images of NAC and (d) SAED pattern of NAC.

rate of 5–100 mV $s^{-1}$ and between the potential of 0 and 0.5 V shown in Figure 9a. The characteristic pseudo-capacitive nature of the electrode can be observed by non-rectangular CV curves [86]. As far as the CV study is concerned, the greater the area under the CV curve at a particular scan rate, the greater the value of specific capacitance will be. It is clear that when the scan rate increases, the CV curve's area grows. Additionally, Figure 9b showed the contribution percentages of diffusion controlled and surface controlled contribution at various scan rates. Even at high scan rates, the diffusion-controlled participation is remarkably steady and higher than the surface-controlled contribution, illustrating that the composite electrode's high capacity mostly results from battery behavior [87].

The galvanostatic charge–discharge analysis is performed to examine the super capacitive behavior of the synthesized composite, GCD curves of all the electrodes was recorded at a current density of 1–50 $Ag^{-1}$ across the potential window of 0 and 0.4 V (Figure 10a) and the corresponding values of specific capacitance are presented in Figure 10b. As current densities rise between 1 and 50 $Ag^{-1}$, electrode's specific capacitance falls. This could be explained by the varying insertion–desertion tendencies of the ions in the electrode and electrolyte materials. These curves exhibit the nonlinear behavior. Hence it is confirmed that the faradaic charge storage mechanism is predominant in the material. At 1 A $g^{-1}$, the highest capacitance of 284.16 C $g^{-1}$ was measured, suggesting improved charge storage. The capacitance decreases with increasing current density. It is the

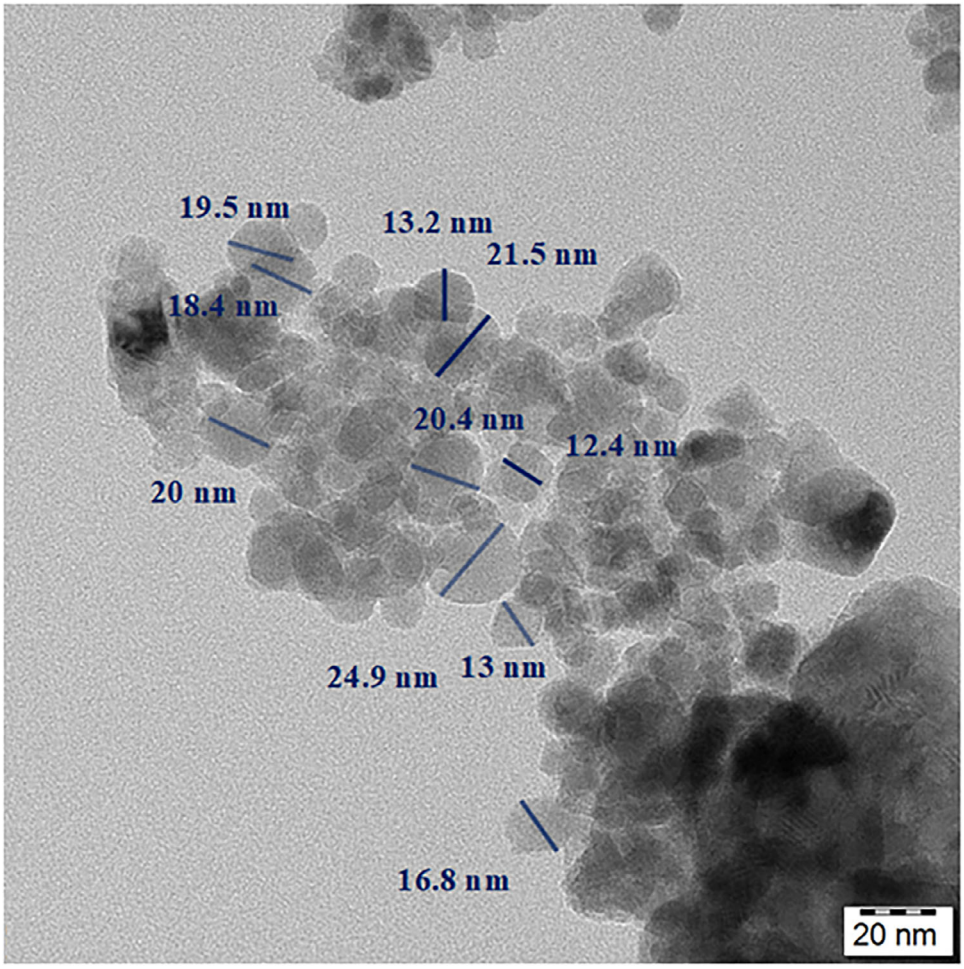


**FIGURE 6** | TEM image of NAC with particle size.

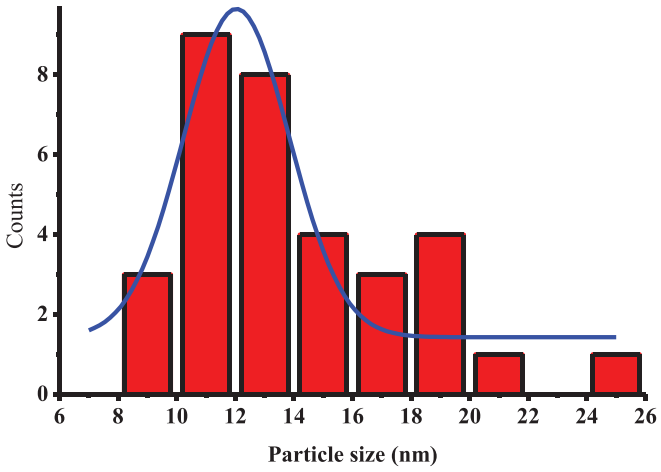


**FIGURE 7** | Particle size distribution histogram of NAC.

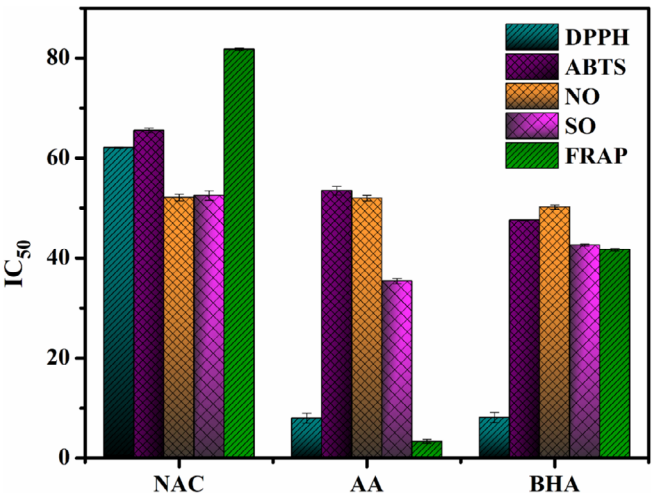


**FIGURE 8** | Antioxidant activity of the NAC.

normal behavior. This may be due that at low current density the rate of diffusion of $OH^-$ ions is high into the electrode, which in turn high capacitance and vice versa.

Furthermore, the EIS method was used to evaluate the electrode's performance; the Nyquist plots that were produced are displayed in Figure 11a. The Nyquist plot is a helpful tool in electrochemical analysis that sheds light on the impedance behavior and electrochemical processes of a system. Three separate zones, each depending on the frequency range under study, are frequently visible on a supercapacitor's Nyquist plot. The intercept value in the high frequency domain indicates the equivalent series resistance (Rs), which is the entire resistance displayed by the

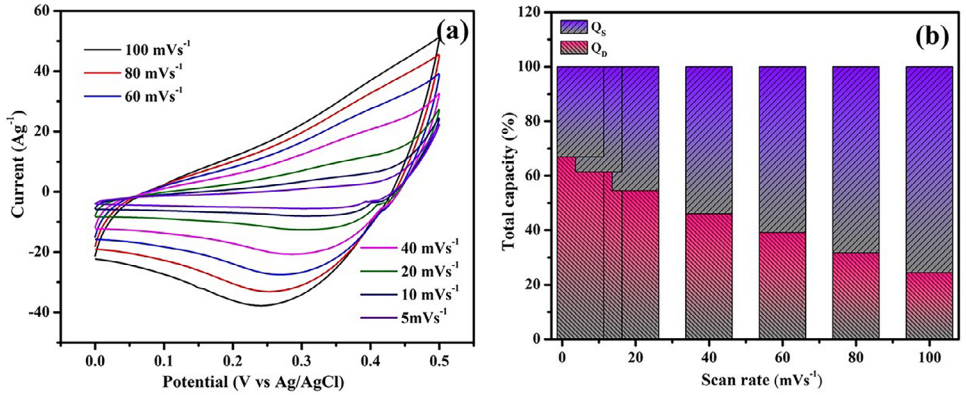


**FIGURE 9** | Electrochemical performances: (a) CV curves and (b) capacitive contributions at various scan rates.

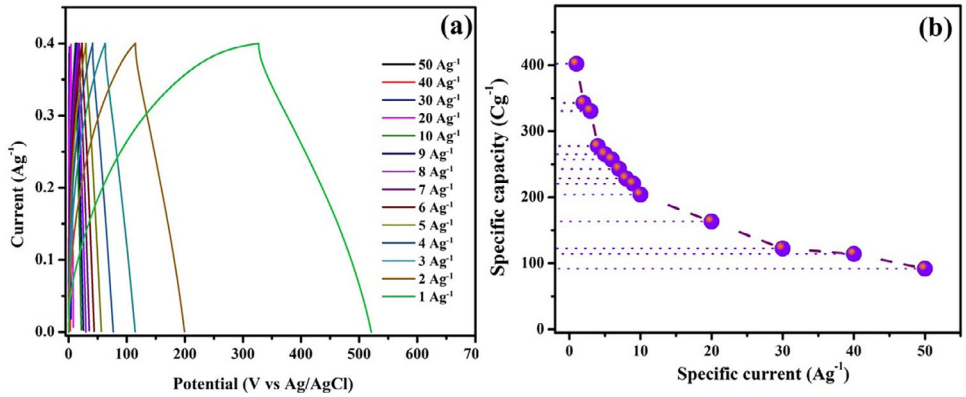


**FIGURE 10** | Electrochemical performances of NAC: (a) GCD curves and (b) specific capacity versus specific currents.

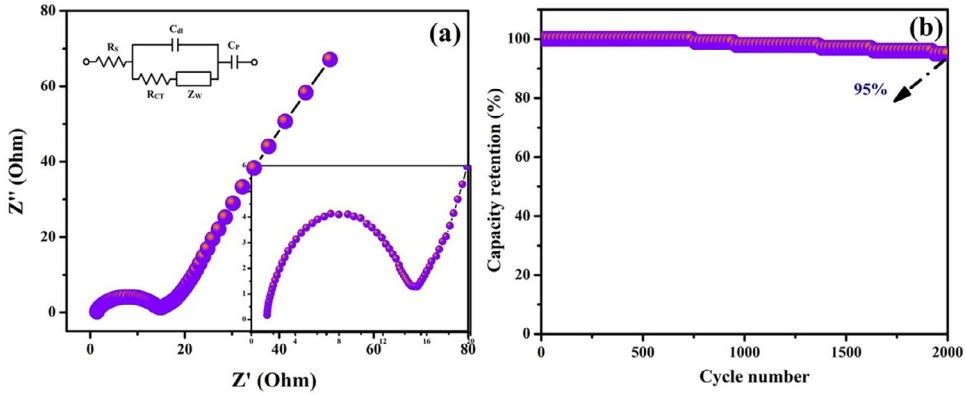


**FIGURE 11** | Electrochemical performance of NAC: (a) Nyquist plot and (b) cyclic stability.

electrolyte, electrode, and electrical connections. Meanwhile, the diameter of the semicircular feature observed in the mid-frequency region is associated with the charge-transfer resistance (Rct) [88, 89]. Warburg impedance, which indicates the diffusion of charge carriers within the electrode material, is indicated in the middle frequency range by an inclination greater than 45° in a linear trend. The electrodes with a smaller semicircle (i.e., Rct) of 1.5 and a lower Rs value of 13.2 are anticipated to perform better in electrochemical energy storage.

One important factor affecting the practicality and viability of supercapacitor electrodes is cyclic stability. This characteristic describes the supercapacitor's ability to maintain their electrochemical efficiency after a large number of cycles of charging and discharging, exhibiting resistance to severe degradation. Therefore, at a current density of 10 $Ag^{-1}$, the stability of the composite electrode was evaluated for 2000 GCD cycles (Figure 11b). After 2000 GCD cycles, the electrode maintained 95% of its initial capacitance, demonstrating good cyclic stability.

Electrochemical application of NAC was compared other previously reported literatures and found significant in the electrochemical applications [90–93].

## 4 | Conclusion

The mixed metal oxide-based NAC of Cu, Zn and Co has been biogenically synthesized using extract of *M. fragrans* (nutmeg) mace and the morphological and chemical formation of the NAC was confirmed and supported by using various characterization techniques like FT-IR, UV–Vis, PXRD, SEM, TEM, and EDS. This NAC was designed to employ a single NAC as the dual applicant in the fields of biomedical and energy, because these fields hold most of the stake quality of life in the lifespan of people. NAC can be opted as a potential candidate for the antioxidant applications which can scavenges most of the free radicals includes, $DPPH^{\bullet}$, $ABTS^{\bullet+}$, $NO^{\bullet}$, FRAP, and $O^{2-}$ with good $IC_{50}$ value. Further, electrochemical candidate NAC delivers quite good results and it can be a high-performance electrode for super capacitors to encounter the demanding energy needs. Conclusively, NAC was a mixed metal nanocomposite synthesized via plant-assisted method and a good applicant for both the energy and biological applications. In near future NAC was yet to be synthesized with series of plant extracts and their electrochemical and biological applications were studied and compared for the better outcomes. Pilot level scale up was planned after the optimization of process protocols for the scalability of NAC. The cornerstone of the future perspective of NAC was to bridge mechanistic clarity with translational applications.


### Acknowledgments

The authors Baskar Anbumani, Giriraj Kalaiarasi, and Ayyar Manikandan are grateful to Karpagam Academy of Higher Education Management for providing research support. The author S. P gratefully acknowledges Department of Science and Technology, New Delhi, India for providing the Women Scientist Scheme- WOS (A) fellowship [Grant No. SR/WOS(A)/CS-147/2021].


### Conflicts of Interest

The authors declare no conflicts of interest.

### Data Availability Statement

The data that support the findings of this study are available in the Supporting Information of this article.

### References


1. N. Joudeh and D. Linke, "Nanoparticle Classification, Physicochemical Properties, Characterization, and Applications: A Comprehensive Review for Biologists," *Journal of Nanobiotechnology* 20 (2022): 1477, https://doi.org/10.1186/s12951-022-01477-8.

2. K. Sreelatha, C. S. AnandaKumar, M. Saraswathi, P. Anusha, N. M. Rose, and D. Bhargava, "A Comprehensive Review of Nanoparticle Characterization Techniques," *International Journal of Research and Review* 12 (2025): 194–200, https://doi.org/10.52403/ijrr.20250124.

3. D. Kirubakaran, J. B. A. Wahid, N. Karmegam, et al., "A Comprehensive Review on the Green Synthesis of Nanoparticles: Advancements in Biomedical and Environmental Applications," *Biomedical Materials & Devices* 4 (2025): 388–413, https://doi.org/10.1007/s44174-025-00295-4.

4. R. Verma, A. B. Khan, A. K. Amar, et al., "Tri-Metallic AM-Ag/CuO/ZnO NC Synthesized via Green Chemistry Principle and Its Biomedical Applications," *Journal of Materials Research* 38 (2023): 4641–4654, https://doi.org/10.1557/s43578-023-01184-6.

5. A. V. Samrot, S. P. R. Singh, R. Deenadhayalan, V. V. Rajesh, S. Padmanaban, and K. Radhakrishnan, "Nanoparticles, a Double-Edged Sword With Oxidant as Well as Antioxidant Properties—A Review," *Oxygen* 2 (2022): 591–604, https://doi.org/10.3390/oxygen2040039.

6. S. Sharma, M. Devi, P. Kumar, et al., "Photocatalytic, Antibacterial and Antioxidant Study of Vitex negundo Mediated Green Synthesized Nickel and Neodymium Doped Zinc Oxide Nanoparticles," *Toxicological & Environmental Chemistry* 107 (2025): 178–206, https://doi.org/10.1080/02772248.2024.2448952.

7. A. Nughwal, R. Bharti, A. Thakur, M. Verma, R. Sharma, and A. Pandey, "Green Synthesis of Iron Oxide Nanoparticles From Mexican Prickly Poppy (Argemone mexicana): Assessing Antioxidant Activity for Potential Therapeutic Use," *RSC Advances* 15 (2025): 10287–10297, https://doi.org/10.1039/D4RA07232D.

8. L. Valgimigli, R. Amorati, and A. Baschieri, "Antioxidant Activity of Nanomaterials," *Journal of Materials Chemistry B* 6 (2018): 2036–2051, https://doi.org/10.1039/c8tb00107c.

9. B. Omran and K.-H. Baek, "Nanoantioxidants: Pioneer Types, Advantages, Limitations, and Future Insights," *Molecules (Basel, Switzerland)* 26 (2021): 7031, https://doi.org/10.3390/molecules26227031.

10. D. R. G. Daré and S. O. S. Lautenschlager, "Nanoparticles With Antioxidant Activity," *Antioxidants* 14 (2025): 221, https://doi.org/10.3390/antiox14020221.

11. I. Khan, H. Hameed, K. Younas, et al., "Unlocking the Power of Antioxidant Nanoparticles: Insights Into Classification, Formulation, Characterization, and Biomedical Applications," *BioNanoScience* 15 (2024): 131, https://doi.org/10.1007/s12668-024-01761-x.

12. G. E. Kılınç and Y. A. Kuru, "Nanotechnology-Based Plant Antioxidants: A Current Literature Review on Bioavailability and Oxidative Stress," *Current Nutrition Reports* 14 (2025): 98, https://doi.org/10.1007/s13668-025-00689-2.

13. U. Pradhan, J. P. Prajapati, P. Majhi, et al., "Green Synthesis and Characterization of Blumea sinuata Silver Nanoparticles: Antibacterial, Antifungal, and Antioxidant Properties," *Nanoscale Advances* 7 (2025): 3732–3745, https://doi.org/10.1039/D4NA01063A.

14. A. H. Al-Hammadi, A. Alnehia, A. Al-Sharabi, H. Alnahari, and A.-B. Al-Odayni, "Synthesis of Trimetallic Oxide ($Fe_2O_3$–MgO–CuO) Nanocomposites and Evaluation of Their Structural and Optical Properties," *Scientific Reports* 13 (2023): 12927, https://doi.org/10.1038/s41598-023-39845-5.

15. S. Iravani and R. S. Varma, "Sustainable Synthesis of Cobalt and Cobalt Oxide Nanoparticles and Their Catalytic and Biomedical Applications," *Green Chemistry* 22 (2020): 2643–2661, https://doi.org/10.1039/d0gc00885k.

16. L. S. Sundar, M. K. Singh, A. M. B. Pereira, and A. C. M. Sousa, "The Cobalt Oxide-Based Composite Nanomaterial Synthesis and Its Biomedical and Engineering Applications," (IntechOpen eBooks, 2019), https://doi.org/10.5772/intechopen.8872.

17. S. R. Bavaji, A. Jafar Ahamed, S. Sadaf, G. M. Alsulaim, and M. W. Alam, "Multifunctional $ZrO_2$/NiO/RGO Ternary Nanocomposites for Degradation of Organic Pollutants, $H_2$ Production and Antioxidant Property," *Journal of Inorganic and Organometallic Polymers and Materials* 35 (2025): 5912–5925, https://doi.org/10.1007/s10904-025-03630-w.

18. N. M. El-Shafai, M. Shukry, I. M. El-Mehasseb, et al., "Electrochemical Property, Antioxidant Activities, Water Treatment and Solar Cell Applications of Titanium Dioxide–Zinc Oxide Hybrid Nanocomposite Based on Graphene Oxide Nanosheet," *Materials Science and Engineering: B* 259 (2020): 114596, https://doi.org/10.1016/j.mseb.2020.114596.

19. J. Khan, S. Bibi, I. Naseem, et al., "Ternary Metal (Cu–Ni–Zn) Oxide Nanocomposite via an Environmentally Friendly Route," *ACS Omega* 8 (2023): 21032–21041, https://doi.org/10.1021/acsomega.3c01896.

20. S. Athithyan, G. Kalaiarasi, S. Parveen, et al., "Facile Synthesis of Cobalt-Nickel Oxide Nanocomposites for Trifunctional Application Towards Antioxidant, Anticancer and Electrochemical Performance," *Inorganic Chemistry Communications* 164 (2024): 112384, https://doi.org/10.1016/j.inoche.2024.112384.

21. A. U. Khan, B. Li, A. O. Alqarni, et al., "Biosynthesis of Silver Capped Magnesium Oxide Nanocomposite Using Olea Cuspidata Leaf Extract and Their Photocatalytic, Antioxidant and Antibacterial Activity," *Photodiagnosis and Photodynamic Therapy* 33 (2020): 102153, https://doi.org/10.1016/j.pdpdt.2020.102153.

22. S. Priyadharshini, A. Thirumurugan, M. Ayyanar, et al., "Sustainable Biogenic Synthesis of High-Performance CaO/NiO Nanocomposite for Antimicrobial, Antioxidant, and Antidiabetic Applications," *Ceramics* 8 (2025): 46, https://doi.org/10.3390/ceramics8020046.

23. R. Papitha, V. Hadkar, N. K. Sishu, S. Arunagiri, S. M. Roopan, and C. I. Selvaraj, "Green Synthesis of CuO/$TiO_2$ and ZnO/$TiO_2$ Nanocomposites Using Parkia Timoriana Bark Extract: Enhanced Antioxidant and Antidiabetic Activities for Biomedical Applications," *Ceramics International* 50 (2024): 39109–39121, https://doi.org/10.1016/j.ceramint.2024.07.277.

24. R. Rai, A. R. Shetty, M. Shree, et al., "Exploring the antimicrobial and antioxidant potential of CuO doped NiO nanocomposites: Synthesis, characterization, and melamine sensing evaluation," *Nanocomposites* 10 (2024): 417–431, https://doi.org/10.1080/20550324.2024.2414137.

25. K. M. Gendo, R. F. Bogale, and G. Kenasa, "Green Synthesis, Characterization, and Evaluation of Photocatalytic and Antibacterial Activities of $Co_3O_4$–ZnO Nanocomposites Using Calpurnia aurea Leaf Extract," *ACS Omega* 9 (2024): 28354–28371, https://doi.org/10.1021/acsomega.4c01595.

26. M. Hariram and S. Vivekanandhan, "Phytochemical Process for the Functionalization of Materials With Metal Nanoparticles: Current Trends and Future Perspectives," *ChemistrySelect* 3 (2018): 13561–13585, https://doi.org/10.1002/slct.201802748.

27. J. Singh, T. Dutta, K.-H. Kim, M. Rawat, P. Samddar, and P. Kumar, "'Green' Synthesis of Metals and Their Oxide Nanoparticles: Applications for Environmental Remediation," *Journal of Nanobiotechnology* 16 (2018): 84, https://doi.org/10.1186/s12951-018-0408-4.

28. S. Ying, Z. Guan, P. C. Ofoegbu, et al., "Green Synthesis of Nanoparticles: Current Developments and Limitations," *Environmental Technology & Innovation* 26 (2022): 102336, https://doi.org/10.1016/j.eti.2022.102336.

29. I. Ahmed, J. A. Banday, and F. A. Mir, "Synthesis of Metal and Metal Oxide Nanoparticles Using Plant Extracts—Characterization and Applications," *BioNanoScience* 13 (2023): 1541–1557, https://doi.org/10.1007/s12668-023-01194-y.

30. A. Bukhari, I. Ijaz, E. Gilani, et al., "Green Synthesis of Metal and Metal Oxide Nanoparticles Using Different Plants' Parts for Antimicrobial Activity and Anticancer Activity: A Review Article," *Coatings* 11 (2021): 1374, https://doi.org/10.3390/coatings11111374.

31. M. Sabitha and D. Helen, "Comparison of Capping Agents Used in Chemical and Green Synthesis of Zinc Oxide Nanoparticles," *International Journal of Interdisciplinary Research Universe* 2 (2022): 9.

32. A. K. Sidhu, N. Verma, and P. Kaushal, "Role of Biogenic Capping Agents in the Synthesis of Metallic Nanoparticles and Evaluation of Their Therapeutic Potential," *Frontiers in Nanotechnology* 3 (2021), https://doi.org/10.3389/fnano.2021.801620.

33. W. Ahmad, A. Pandey, V. Rajput, V. Kumar, M. Verma, and H. Kim, "Plant Extract Mediated Cost-Effective Tin Oxide Nanoparticles: A Review on Synthesis, Properties, and Potential Applications," *Current Research in Green and Sustainable Chemistry* 4 (2021): 100211, https://doi.org/10.1016/j.crgsc.2021.100211.

34. K. K. Kadimpati and N. Golla, "Cost-Effective Biogenic-Production of Inorganic Nanoparticles, Characterizations, and Their Antimicrobial Properties," (2022): 265–290, https://doi.org/10.1016/B978-0-12-822933-0.00017-6.

35. V. Kuete, "*Myristica fragrans*: A Review," *Elsevier eBooks* (2017): 497–512, https://doi.org/10.1016/B978-0-12-809286-6.00023-6.

36. M. R. Loizzo, V. Sicari, M. C. Tenuta, et al., "Phytochemicals Content, Antioxidant and Hypoglycaemic Activities of Commercial Nutmeg mace ( *Myristica fragrans* L.) and Pimento ( Pimenta dioica (L.) Merr.)," *International Journal of Food Science & Technology* 51 (2016): 2057–2063, https://doi.org/10.1111/ijfs.13178.

37. G. I. Edo, A. N. Mafe, A. B. M. Ali, et al., "Green Biosynthesis of Nanoparticles Using Plant Extracts: Mechanisms, Advances, Challenges, and Applications," *BioNanoScience* 15 (2025): 267, https://doi.org/10.1007/s12668-025-01883-w.

38. N. S. Alsaiari, F. M. Alzahrani, A. Amari, et al., "Plant and Microbial Approaches as Green Methods for the Synthesis of Nanomaterials: Synthesis, Applications, and Future Perspectives," *Molecules (Basel, Switzerland)* 28 (2023): 463, https://doi.org/10.3390/molecules28010463.

39. M. Thaha, J. H. J. Manohar, and A. Rajasekar, "Green Synthesis and In Vitro Insights of Zinc Oxide Nanoparticles Using Nutmeg and Flaxseed Extracts," *Pharmacognosy Research* 17 (2025): 816–822, https://doi.org/10.5530/pres.20252068.

40. Z. Villagrán, L. M. Anaya-Esparza, C. A. Velázquez-Carriles, et al., "Plant-Based Extracts as Reducing, Capping, and Stabilizing Agents for the Green Synthesis of Inorganic Nanoparticles," *Resources* 13 (2024): 70, https://doi.org/10.3390/resources13060070.

41. R. Re, N. Pellegrini, A. Proteggente, A. Pannala, M. Yang, and C. Rice-Evans, "Antioxidant Activity Applying an Improved ABTS Radical Cation Decolorization Assay," *Free Radical Biology and Medicine* 26 (1999): 1231–1237, https://doi.org/10.1016/S0891-5849(98)00315-3.

42. X. Liang, L. Shi, R. Zhang, and M. Zhang, "Pectin-Mediated Green Synthesis of CuO Nanoparticles: Evaluation of Its Cytotoxicity, Antioxidant and Anti-Human Cervical Cancer Properties," *Journal of Experimental Nanoscience* 17 (2022): 315–325, https://doi.org/10.1080/17458080.2021.2013470.

43. W. Fu, J. Chen, Y. Cai, et al., "Antioxidant, Free Radical Scavenging, Anti-Inflammatory and Hepatoprotective Potential of the Extract From Parathelypteris Nipponica (Franch. et Sav.) Ching," *Journal of Ethnopharmacology* 130 (2010): 521–528, https://doi.org/10.1016/j.jep.2010.05.039.

44. B. M. Olabinri, O. O. Odedire, T. M. Olaleye, A. S. Adekunl, L. O. Ehigie, and O. Folashade, "In Vitro Evaluation of Hydroxyl and Nitric Oxide Radical Scavenging Activities of Artemether," *Research Journal of Biological Sciences* 5 (2010): 102–105, https://doi.org/10.3923/rjbsci.2010.102.105.

45. T.-R. Li, Z.-Y. Yang, B.-D. Wang, and D.-D. Qin, "Synthesis, Characterization, Antioxidant Activity and DNA-Binding Studies of Two Rare Earth(III) Complexes With Naringenin-2-Hydroxy Benzoyl Hydrazone Ligand," *European Journal of Medicinal Chemistry* 43 (2007): 1688–1695, https://doi.org/10.1016/j.ejmech.2007.10.006.

46. E. Gobinath, M. Dhatchinamoorthy, P. Saran, D. Vishnu, R. Indumathy, and G. Kalaiarasi, "Synthesis and Characterization of NiO Nanoparticles Using Sesbania Grandiflora Flower to Evaluate Cytotoxicity," *Results in Chemistry* 6 (2023): 101043, https://doi.org/10.1016/j.rechem.2023.101043.

47. H. Abramovič, B. Grobin, N. P. Ulrih, and B. Cigić, "Relevance and Standardization of In Vitro Antioxidant Assays: ABTS, DPPH, and Folin–Ciocalteu," *Journal of Chemistry* 2018 (2018): 1–9, https://doi.org/10.1155/2018/4608405.

48. G. Aldini, A. Altomare, G. Baron, et al., "*N*-Acetylcysteine as an Antioxidant and Disulphide Breaking Agent: The Reasons Why," *Free Radical Research* 52 (2018): 751–762, https://doi.org/10.1080/10715762.2018.1468564.

49. F. Shahidi and A. Samarasinghe, "How to Assess Antioxidant Activity? Advances, Limitations, and Applications of In Vitro, In Vivo, and Ex

Vivo Approaches," *Food Production, Processing and Nutrition* 7 (2025): 50, https://doi.org/10.1186/s43014-025-00326-z.

50. N. B. Sadeer, D. Montesano, S. Albrizio, G. Zengin, and M. F. Mahomoodally, "The Versatility of Antioxidant Assays in Food Science and Safety—Chemistry, Applications, Strengths, and Limitations," *Antioxidants* 9 (2020): 709, https://doi.org/10.3390/antiox9080709.

51. H. Assefa and E. Adane, "Enhanced Electrochemical Performance of $CuV_2O_6$/GCN Nanocomposite as a High-Performance Supercapacitor Electrode," *Journal of Materials Science: Materials in Electronics* 36 (2025): 1624, https://doi.org/10.1007/s10854-025-15689-9.

52. M. Devi, J. Shikhar, and S. Sharma, "Effect of Nitrogen Content on Performance of Supercapacitors Composed of Nitrogen–carbon Materials," *Journal of Materials Chemistry A* 13 (2025): 42343–42354, https://doi.org/10.1039/d5ta06469d.

53. Y. Kumar, S. Sharma, and V. S. R. Rajasekhar Pullabhotla, "Electrochemical Characterizations of Electrode Materials for Supercapacitors," *Materials* 7 (2025): 10, https://doi.org/10.33263/Materials71.010.

54. S. M. Mousavi, S. A. Hashemi, S. Ramakrishna, et al., "Green Synthesis of Supermagnetic $Fe_3O_4$–MgO Nanoparticles via Nutmeg Essential Oil Toward Superior Anti-Bacterial and Anti-Fungal Performance," *Journal of Drug Delivery Science and Technology* 54 (2019): 101352, https://doi.org/10.1016/j.jddst.2019.101352.

55. N. R. Putra, A. H. A. Aziz, H. Mamat, et al., "Green Extraction of Nutmeg (*Myristica fragrans*) Phytochemicals: Prospective Strategies and Roadblocks," *Open Agriculture* 9 (2024): 20220285, https://doi.org/10.1515/opag-2022-0285.

56. M. Ovais, A. T. Khalil, N. U. Islam, et al., "Role of Plant Phytochemicals and Microbial Enzymes in Biosynthesis of Metallic Nanoparticles," *Applied Microbiology and Biotechnology* 102 (2018): 6799–6814, https://doi.org/10.1007/s00253-018-9146-7.

57. Y. Khane, Z. Hafsi, F. Fenniche, et al., "Green Synthesis of Zinc Oxide Nanoparticles Using *Lepidium sativum* Seed Extract Embedded in Sodium Alginate Matrix for Efficient Slow-Release Biofertilizers," *Multidisciplinary Digital Institute* 67 (2024): 35, https://doi.org/10.3390/engproc2024067035.

58. W. Abd-Elhamed, A. A. Mohamed, Z. H. Saad, S. E.-S. I. Hassanien, M. Z. M. Salem, and M. El-Hefny, "Green Synthesis of Silver Nanoparticles Mediated by Solanum Nigrum Leaf Extract and Their Antifungal Activity Against Pine Pathogens," *Scientific Reports* 15 (2025): 35025, https://doi.org/10.1038/s41598-025-21291-0.

59. S. Magar, S. Bhartal, S. Bhendekar, P. Bhosale, S. Bodhak, and S. Bramharakshas, "Green Synthesis of Metal Nanoparticles Using Plant Extracts," *International Journal of Pharmaceutical Sciences* 3 (2025): 1315–1318, https://doi.org/10.5281/zenodo.15611246.

60. T. Sarathamani, V. Kalaiselvi, B. Blessymol, et al., "Annona Squamosa Seeds Capped Calcium Oxide Nanoparticles: Antimicrobial, Antioxidant, Anti-Ulcer Analysis," *RSC Advances* 15 (2025): 4904–4914, https://doi.org/10.1039/d5ra00375j.

61. L. Castillo-Henríquez, K. Alfaro-Aguilar, J. Ugalde-Álvarez, L. Vega-Fernández, G. Montes de Oca-Vásquez, and J. R. Vega-Baudrit, "Green Synthesis of Gold and Silver Nanoparticles From Plant Extracts and Their Possible Applications as Antimicrobial Agents in the Agricultural Area," *Nanomaterials* 10 (2020): 1763, https://doi.org/10.3390/nano10091763.

62. H. Rizwana, N. A. Bokahri, F. S. Alkhattaf, G. Albasher, and H. A. Aldehaish, "Antifungal, Antibacterial, and Cytotoxic Activities of Silver Nanoparticles Synthesized From Aqueous Extracts of Mace-Arils of *Myristica fragrans*," *Molecules (Basel, Switzerland)* 26 (2021): 7709, https://doi.org/10.3390/molecules26247709.

63. C. Vanlalveni, S. Lallianrawna, A. Biswas, M. Selvaraj, B. Changmai, and S. L. Rokhum, "Green Synthesis of Silver Nanoparticles Using Plant Extracts and Their Antimicrobial Activities: A Review of Recent Literature," *RSC Advances* 11 (2021): 2804–2837, https://doi.org/10.1039/d0ra09941d.

64. Annu, M. Sahu, S. Singh, S. Prajapati, D. K. Verma, and D. K. Shin, "From Green Chemistry to Biomedicine: The Sustainable Symphony of Cobalt Oxide Nanoparticles," *RSC Advances* 14 (2024): 32733–32758, https://doi.org/10.1039/d4ra05872k.

65. N. Ahmed, Z. Khalil, Z. Farooq, et al., "Structural, Optical, and Magnetic Properties of Pure and Ni–Fe-Codoped Zinc Oxide Nanoparticles Synthesized by a Sol–Gel Autocombustion Method," *ACS Omega* 9 (2023): 137–145, https://doi.org/10.1021/acsomega.3c01727.

66. P. Bindu and S. Thomas, "Estimation of Lattice Strain in ZnO Nanoparticles: X-Ray Peak Profile Analysis," *Journal of Theoretical and Applied Physics* 8 (2014): 123–134, https://doi.org/10.1007/s40094-014-0141-9.

67. A. K. Zak, W. H. Abd Majid, M. E. Abrishami, and R. Yousefi, "X-Ray Analysis of ZnO Nanoparticles by Williamson–Hall and Size–strain Plot Methods," *Solid State Sciences* 13 (2010): 251–256, https://doi.org/10.1016/j.solidstatesciences.2010.11.024.

68. S. Velumani, S. K. Narayandass, and D. Mangalaraj, "Structural Characterization of Hot Wall Deposited Cadmium Selenide Thin Films," *Semiconductor Science and Technology* 13 (1998): 1016–1024, https://doi.org/10.1088/0268-1242/13/9/009.

69. D. H. Manh, T. T. N. Nha, L. T. H. Phong, P. H. Nam, T. D. Thanh, and P. T. Phong, "Determination of the Crystalline Size of Hexagonal La1−xSrxMnO$_3$ (x = 0.3) Nanoparticles From X-Ray Diffraction—a Comparative Study," *RSC Advances* 13 (2023): 25007–25017, https://doi.org/10.1039/D3RA04018F.

70. M. S. H. Bhuiyan, M. Y. Miah, S. C. Paul, et al., "Green Synthesis of Iron Oxide Nanoparticle Using Carica papaya Leaf Extract: Application for Photocatalytic Degradation of Remazol Yellow RR Dye and Antibacterial Activity," *Heliyon* 6 (2020): e04603, https://doi.org/10.1016/j.heliyon.2020.e04603.

71. M. Zeb, Z. Anjum, S. Mumtaz, M. Khalid, and M. Hafeez, "*Jasminum mesyni* Mediated Synthesis of $Co_3O_4$/NiO Nanocomposite for Methylene Blue Degradation," *Desalination and Water Treatment* 317 (2024): 100165, https://doi.org/10.1016/j.dwt.2024.100165.

72. E. N. Frankel and A. S. Meyer, "The Problems of Using One-Dimensional Methods to Evaluate Multifunctional Food and Biological Antioxidants," *Journal of the Science of Food and Agriculture* 80 (2000): 1925–1941, https://doi.org/10.1002/1097-0010(200010)80:13.

73. A. Gupta, R. Jamatia, R. A. Patil, Y.-R. Ma, and A. K. Pal, "Copper Oxide/Reduced Graphene Oxide Nanocomposite-Catalyzed Synthesis of Flavanones and Flavanones With Triazole Hybrid Molecules in One Pot: A Green and Sustainable Approach," *ACS Omega* 3 (2018): 7288–7299, https://doi.org/10.1021/acsomega.8b00334.

74. K. J. Davies, "Protein Damage and Degradation by Oxygen Radicals. I. General Aspects," *Journal of Biological Chemistry* 262 (1987): 9895–9901, https://doi.org/10.1016/s0021-9258(18)48018-0.

75. A. S. Eltaweil, A. M. Abdelfatah, M. Hosny, and M. Fawzy, "Novel Biogenic Synthesis of a Ag@Biochar Nanocomposite as an Antimicrobial Agent and Photocatalyst for Methylene Blue Degradation," *ACS Omega* 7 (2022): 8046–8059, https://doi.org/10.1021/acsomega.1c07209.

76. S. Ali, K. G. Sudha, N. Thirumalaivasan, et al., "Green Synthesis of Magnesium Oxide Nanoparticles by Using Abrus precatorius Bark Extract and Their Photocatalytic, Antioxidant, Antibacterial, and Cytotoxicity Activities," *Bioengineering* 10 (2023): 302, https://doi.org/10.3390/bioengineering10030302.

77. M. Afifi, N. M. Kadasa, and O. A. Almaghrabi, "Ameliorative Effect of Zinc Oxide Nanoparticles on Antioxidants and Sperm Characteristics in Streptozotocin-Induced Diabetic Rat Testes," *BioMed Research International* 2015 (2015): 1–6, https://doi.org/10.1155/2015/153573.

78. S. Haq, H. Afsar, M. Ben Ali, M. Almalki, B. Albogami, and A. Hedf, "Green Synthesis and Characterization of a ZnO-$ZrO_2$ Heterojunction for Environmental and Biological Applications," *Crystals* 11 (2021): 1502, https://doi.org/10.3390/cryst11121502.

79. G. Nikaeen, S. Yousefinejad, S. Rahmdel, F. Samari, and S. Mahdavinia, "Central Composite Design for Optimizing the Biosynthesis of Silver Nanoparticles Using Plantago Major Extract and Investigating Antibacterial, Antifungal and Antioxidant Activity," *Scientific Reports* 10 (2020): 9642, https://doi.org/10.1038/s41598-020-66357-3.

80. P. C. Mali, N. Bharti, P. Yadav, and A. K. Kansotiya, "An Antioxidant Potential Analysis of Herbal Silver Nanoparticles Synthesized From Methanolic Leaf Extract of Cassia siamea," *IP International Journal of Comprehensive and Advanced Pharmacology* 9 (2024): 275–283, https://doi.org/10.18231/j.ijcaap.2024.040.

81. J. A. A. Abdullah, M. Jiménez-Rosado, V. Perez-Puyana, A. Guerrero, and A. Romero, "Green Synthesis of FexOy Nanoparticles With Potential Antioxidant Properties," *Nanomaterials* 12 (2022): 2449, https://doi.org/10.3390/nano12142449.

82. V. Jadhav, A. Bhagare, I. H. Ali, et al., "Role of Moringa Oleifera on Green Synthesis of Metal/Metal Oxide Nanomaterials," *Journal of Nanomaterials* 2022 (2022): 2147393, https://doi.org/10.1155/2022/2147393.

83. J. Vera, W. Herrera, E. Hermosilla, et al., "Antioxidant Activity as an Indicator of the Efficiency of Plant Extract-Mediated Synthesis of Zinc Oxide Nanoparticles," *Antioxidants* 12 (2023): 784, https://doi.org/10.3390/antiox12040784.

84. B. P. G. Bhavyasree and T. S. Xavier, "Green Synthesised Copper and Copper Oxide Based Nanomaterials Using Plant Extracts and Their Application in Antimicrobial Activity: Review," *Current Research in Green and Sustainable Chemistry* 5 (2021): 100249, https://doi.org/10.1016/j.crgsc.2021.100249.

85. A. Geremew, L. Carson, S. Woldesenbet, et al., "Effect of Zinc Oxide Nanoparticles Synthesized From *Carya illinoinensis* Leaf Extract on Growth and Antioxidant Properties of Mustard (Brassica juncea)," *Frontiers in Plant Science* 14 (2023): 1108186, https://doi.org/10.3389/fpls.2023.1108186.

86. C. Wu, K. Zhang, Y. Zhu, and J. Cai, "Hybrid Reduced Graphene Oxide Nanosheet Supported Mn–Ni–Co Ternary Oxides for Aqueous Asymmetric Supercapacitors," *ACS Applied Materials & Interfaces* 9 (2017): 19114–19123, https://doi.org/10.1021/acsami.7b03709.

87. M. Konwar, L. J. Borthakur, and R. S. K. Singh, "Zinc Cobalt Sulfide/Reduced Graphene Oxide Nanocomposite for High-Performance Asymmetric Supercapacitor: A Microwave-Assisted Synthesis," *Energy Technology* 12 (2024): 2301524, https://doi.org/10.1002/ente.202301524.

88. F. Wang, Z. Jia, Y. Zhu, T. Zhang, J. Cheng, and X. Zhao, "Preparation of High Specific Surface Area Porous Carbon From Waste Bamboo fiber for High Performance Supercapacitors," *Biomass and Bioenergy* 202 (2025): 108253, https://doi.org/10.1016/j.biombioe.2025.108253.

89. A. Alaghmandfard and K. Ghandi, "A Comprehensive Review of Graphitic Carbon Nitride (g-C3N4)–Metal Oxide-Based Nanocomposites: Potential for Photocatalysis and Sensing," *Nanomaterials* 12 (2022): 294, https://doi.org/10.3390/nano12020294.

90. S. Yadav, N. Rani, and K. Saini, "Green Synthesis of ZnO and CuO NPs Using Ficus Benghalensis Leaf Extract and Their Comparative Study for Electrode Materials for High Performance Supercapacitor Application," *Materials Today: Proceedings* 49 (2021): 2124–2130, https://doi.org/10.1016/j.matpr.2021.08.323.

91. I. L. Ikhioya, E. U. Onoh, A. C. Nkele, et al., "The The Green Synthesis of Copper Oxide Nanoparticles Using the Moringa Oleifera Plant and its Subsequent Characterization for Use in Energy Storage Applications," *East European Journal of Physics* 1 (2023): 162–172, https://doi.org/10.26565/2312-4334-2023-1-20.

92. Y. Liu and G. Liu, "Green Synthesis and Electrochemical Performances of ZnO/Graphene Nanocomposites," *Ionics* 28 (2022): 3547–3555, https://doi.org/10.1007/s11581-022-04571-x.

93. J. Meena, N. Kumaraguru, N. S. Veerappa, et al., "Copper Oxide Nanoparticles Fabricated by Green Chemistry Using Tribulus Terrestris Seed Natural Extract-Photocatalyst and Green Electrodes for Energy Storage Device," *Scientific Reports* 13 (2023): 22499, https://doi.org/10.1038/s41598-023-49706-w.

## Supporting Information

Additional supporting information can be found online in the Supporting Information section.

The UV–Vis spectroscopic data of the NAC and antioxidant assay graphs have been given in the Supporting Information.

**Supporting File:** slct72668-sup-0001-SuppMat.docx.